The EMBO Journal vol.4 no.13B pp.3661-3665, 1985

Image reconstruction of the Alzheimer paired helical filament

R.A.Crowther and C.M.Wischik[1]

Medical Research Council Laboratory of Molecular Biology, Hills Road, Cambridge CB2 2QH, and [1]Department of Psychiatry, University of Cambridge, Clinical School, Hills Road, Cambridge CB2 2QQ, UK

Communicated by R.A.Crowther

The paired helical filament (PHF) is the principal constituent of the neurofibrillary tangles that occur in the brain in senile dementias of the Alzheimer type. We have previously shown from fragmentation patterns of isolated PHFs that they consist of a regularly repeating subunit, which is axially compact and not an extended fibrous molecule or protofilament. Here we present diffraction patterns of PHFs and an objective reconstruction of the cross-sectional density of the PHF computed from the diffraction patterns. We demonstrate the presence of an axial periodicity (3 nm) in PHFs. These results establish conclusively that the PHF is made up of a double helical stack of transversely oriented subunits, each of which has three domains, and precludes purely descriptive models based on helical rearrangements of preformed cytoskeletal polymers or protofilaments. The structure is of the type that might arise by the *de novo* assembly of a single structural subunit, which appears to be produced in considerable abundance in those neurons where tangles form.

Key words: Alzheimer's disease/paired helical filaments/tangles/image reconstruction

Introduction

Senile dementia of the Alzheimer type is an age-related disorder, affecting some 4% of those aged over 65 in the UK, and is associated with specific neuropathological lesions (Tomlinson, 1982). Strong statistical correlations have been established between the degree of dementia observed in life and the formation of neurofibrillary tangles and neuritic plaques in the cerebral cortex and hippocampus (Roth *et al.*, 1967; Blessed *et al.*, 1968; Roth, 1971; Wilcock and Esiri, 1982). Tangles represent dense accumulations of an ultrastructurally distinct paired helical filament (PHF) (Kidd, 1963; Wisniewski *et al.*, 1976, 1979) and it is significant that the same filaments are also found to accumulate in the abnormal neuritic processes of the plaque (Kidd, 1964; Wisniewski and Terry, 1970). Intermediate filament aggregates have been observed to form in the cell perikaryon after microtubule depolymerisation (Goldman *et al.*, 1979). It is not clear whether the formation of tangles is analogous (Sato *et al.*, 1982) and thus whether tangles arise from the collapse and possible eventual cross-linking of preformed cytoskeletal elements, such as neurofilaments (Metuzals *et al.*, 1981; Selkoe *et al.*, 1982a). There have been reports that antibodies raised against neurofilaments label tangles (Ihara *et al.*, 1981; Anderton *et al.*, 1982; Gambetti *et al.*, 1983), although neurofilament cross-reactivity is lost after mild tangle extraction (Bignami *et al.*, 1984). The immunocytochemical results are presently difficult to interpret. The biochemical approach has been similarly problematical. It was initially reported that tangle extracts contain an abnormal 50-kd band on SDS gels (Iqbal *et al.*, 1974) and, more recently, a 62-kd and a 57-kd band (Iqbal *et al.*, 1984). However, other studies have suggested that the tangle proteins are SDS insoluble (Selkoe *et al.*, 1982b). Most recently it has been claimed that tangles contain a 4-kd peptide, the N-terminal sequence of which is the same as the amyloid of plaque cores and blood vessels (Masters *et al.*, 1985).

If tangles are formed by the collapse or rearrangement of preformed cytoskeletal elements, it should be possible to discern a structural similarity between the PHF and known cytoskeletal polymers. We have prepared tangle-enriched fractions in non-denaturing conditions (Wischik *et al.*, 1985), so as to permit the visualization of individual PHFs by negative staining. The lack of straightness and variability of helical twist complicates the use of reconstruction techniques to analyse the subunit structure of

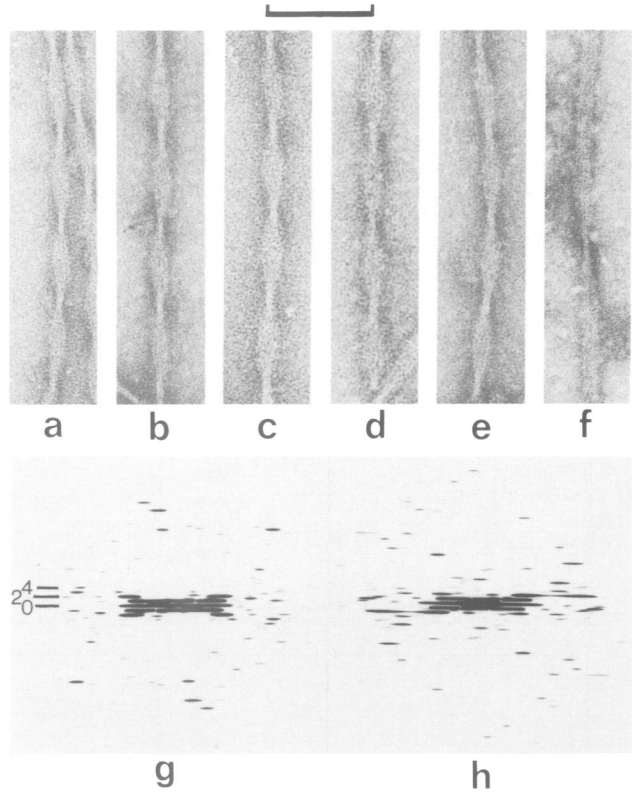

Fig. 1. (a)-(f) Electron micrographs of paired helical filaments, negatively stained with lithium phosphotungstate. The filaments **(a)-(e)** are in a native conformation. The untwisted ribbon-like fragment in **(f)** results from treatment of PHFs on the grid with strong alkali (0.1 M LiOH). Approximate magnification × 140 000. Scale bar 100 nm.
(g)-(h) Computed diffraction patterns (Fourier transforms) of the particles shown in **(a)** and **(b)**. The images were straightened and re-interpolated to constant loop length (see Materials and methods) prior to computing the transforms. The first four layer lines of the 80-nm cross-over spacing are indicated. The other features in the pattern are not consistent from image to image.

the PHF. However, by re-interpolation of the images we have managed to recover sufficient information to compute a cross-sectional map of the PHF. By using autocorrelation functions we have also detected a 3-nm axial spacing in PHFs, which we tentatively ascribe to the subunit spacing. The results, already described in a preliminary abstract (Crowther *et al.*, 1985), appear to exclude models of the PHF based on simple rearrangements of preformed cytoskeletal elements or their constituent protofilaments.

Results

The images of PHFs (Figure 1) show alternating loops (~20 nm wide) and cross-overs (~8 nm wide) with an apparent repeat of ~80 mm (Wisniewski *et al.*, 1984), typical of a twisted ribbon-like structure (Wischik *et al.*, 1985). The spacing between cross-overs is quite variable and Figure 2 shows a histogram of loop lengths measured from a number of filaments in several different fields. The lengths vary from ~65 nm to >100 nm with a mean of 79 nm. The distribution is a fair reflection of the variability both within an individual filament and between different filaments. The histogram is quite skew with a tail to longer loop lengths, reflecting the ability of the PHF to untwist, an effect seen most markedly on alkali treatment which produces flat ribbons (Figure 1f) (Wischik *et al.*, 1985). The variability of twist makes it difficult to produce good optical diffraction patterns. However, it is possible partially to overcome this difficulty by re-interpolating the images so as to straighten them and to produce loops of constant length (Materials and methods). This procedure leads to computed diffraction patterns (Figure 1g,h), which generally show the first four and occasionally the fifth layer lines of the 80-nm cross-over spacing.

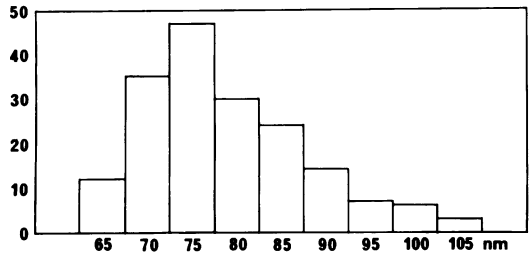

Fig. 2. Histogram showing distribution of loop lengths in negatively stained PHFs. The distribution has a tail to longer loop lengths, indicating a propensity to unwind, seen most dramatically in the flat ribbons produced by alkali treatment.

Comparison of the phases of peaks across the meridian indicates that the Bessel functions occurring on all these layer lines are of even order, as expected at low resolution for a double helical structure. Accordingly we assign Bessel orders $n=2$, 4, 6 and 8, respectively, to layer lines 1–4. The averaged layer line data from the five particles shown in Figure 1a–e are plotted in Figure 3. From these data a cross-section of the PHF (Figure 4a) can then be computed by a standard Fourier program for helical particles (DeRosier and Moore, 1970; Amos, 1975). Similar results were obtained using data from individual transforms (Figure 1g,h) but the reconstruction from the averaged data was less noisy and hence more reliable. With only low order layer lines contributing to the reconstruction, there is little modulation in the axial direction in the computed map. We therefore show only a single section, which nevertheless gives a good idea of the cross-sectional distribution of matter. We have also used the data to resynthesize an image of a PHF projected normal to the axis (Figure 4b). Although axially smeared, this clearly demonstrates the pattern of longitudinal features that we previously analysed by model building (Wischik *et al.*, 1985).

The structural subunit appears to consist of three domains; the inner ones closest to the axis are ~3.5 nm in diameter, while

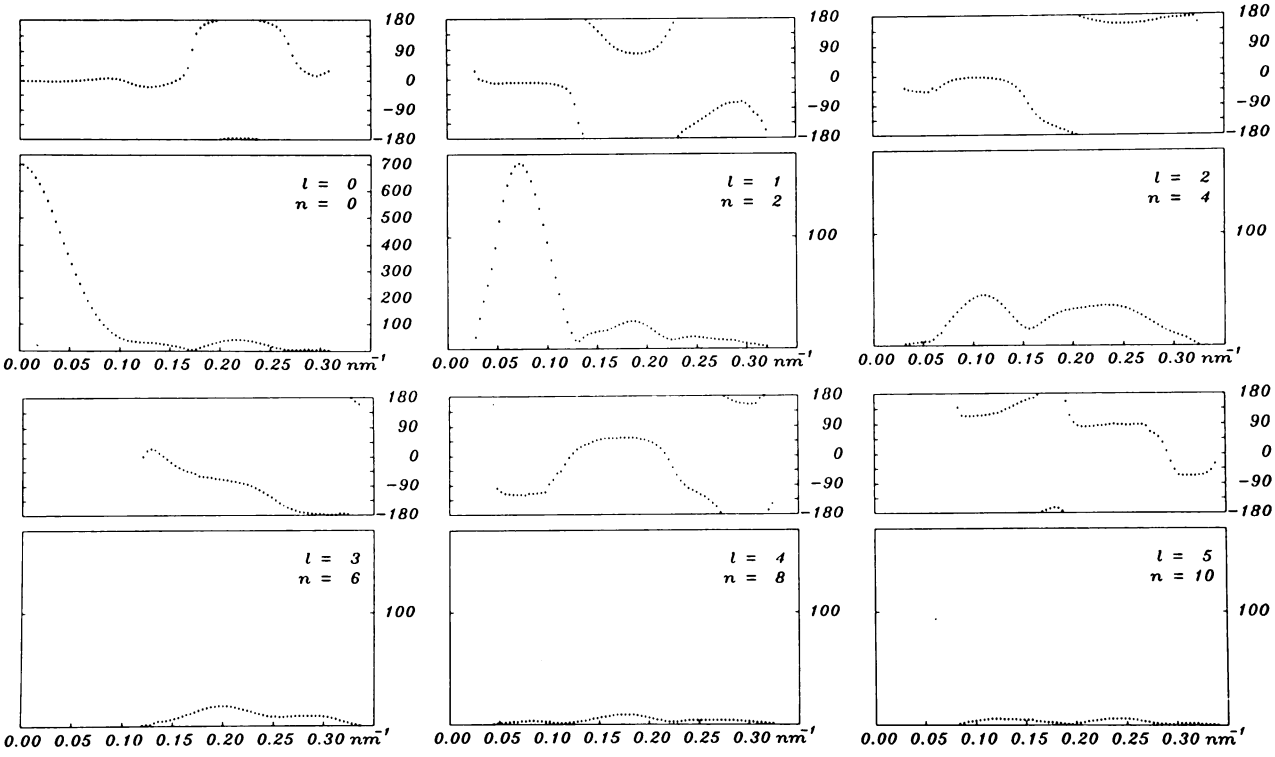

Fig. 3. Average layer line data from the particles shown in Figure 1(a)–(e). In each panel the lower box represents the amplitude plotted as a function of spatial frequency along layer line ℓ, while the upper box represents the phase in degrees. The Bessel function order assigned to each layer line is denoted by n.

the outer is more ellipsoidal with approximate dimensions 3.5 nm × 6.5 nm. The domains are arranged to produce a C-shaped subunit with a deep central cleft. We favour this apportioning of domains to the subunits because of the appearance of the single-stranded regions of PHFs previously observed (Wischik *et al.*, 1985). These images indicate that the strands come apart in the region of contact between the two Cs. The stain-excluding regions give the PHF an elongated cross-section of dimensions 8 nm × 20 nm.

A number of the images of PHFs do show hints of transverse striping (Wischik *et al.*, 1985) with a spacing of 3 – 4 nm. However, this striping is generally seen only in part of the loop and seldom in adjacent loops, so that the pattern is insufficiently ordered to generate higher order layer lines in diffraction patterns. Similar striping is seen in flat ribbons (Figure 1f) produced by alkali treatment of PHFs, though this is also disordered. Even though such disordered spacings do not show up clearly in diffraction patterns, they can nevertheless be detected by generating from the original image its autocorrelation function, which displays the dominant vector spacings. This can be done optically (Elliott *et al.*, 1969) but is now more conveniently carried out digitally by Fourier inversion of the intensity distribution in the Fourier transform of the image, as in the case of computing the Patterson function in X-ray crystallography. Both auto-correlation functions (Figure 5a,b) of the images (Figure 1e,f) show, besides the dominant origin peak, a centrosymmetrically related pair of peaks which correspond to axial spacings of ~3 nm.

Discussion

The results presented here, taken in conjunction with our previous morphological study (Wischik *et al.*, 1985), establish that the PHF consists of two structural strands of subunits. The distribution of matter in these subunits gives the filament an elongated cross-section. The changing aspect produced by the helical arrangement of the subunits then gives the wide to narrow modulation in diameter which is characteristic of the images of PHFs. Each subunit is axially compact and it is likely that the 3-nm axial spacing we have detected corresponds to the axial repeat of the subunit. The arrangement of the three domains within the subunit gives it an overall C-shape, with a large central cleft. From our previous observations of single-stranded regions, it is unlikely that this cleft represents a subunit boundary. Rather, when the two strands separate, the cleavage appears to occur in the region of contact between the two C-shaped features, establishing them as structural subunits. The volume of stain-excluding material makes it likely that the structural subunit has a mol. wt. > 200 kd.

The lining up in an axial direction of domains in neighbouring structural subunits gives rise to the tram-line appearance within each loop noted previously (Wischik *et al.*, 1985) and shown clearly in the projected image (Figure 4b). This appearance has been described as four protofilaments (Wisniewski *et al.*, 1984) or as arising from the overlap of eight protofilaments consisting of globules connected by longitudinal bars (Wisniewski and Wen, 1985). Our observations of sharp transverse breaks and absence of fraying, even in untwisted filaments, and the present map of the subunit density, are inconsistent with such a description of the structure in terms of protofilaments. The pattern of three and four longitudinal stripes within a loop is produced by the helical symmetry, which leads to a changing superposition of the domains within the rotated subunits when these are viewed in projection (Figure 4b).

Our current view of the structure is summarized in the model shown in Figure 6a. The transform of this model (Figure 6b) emphasises the difficulty likely to be encountered in indexing the diffraction patterns, even if the images were of well preserved and regular structures. Thus, besides the group of low order layer

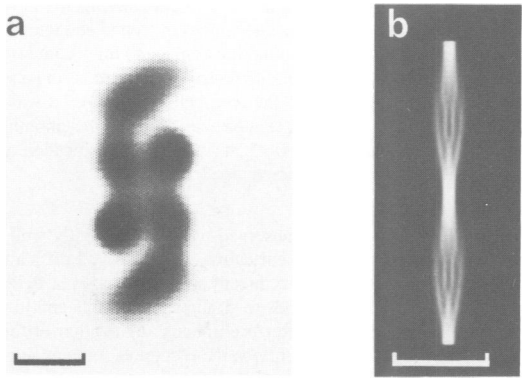

Fig. 4. **(a)** Reconstructed cross-section of the paired helical filament. The map was calculated from the layer lines shown in Figure 3, including data out to a radial cut-off of ~1/3 nm^{-1}. The section was computed using standard helical reconstruction programs (DeRosier and Moore, 1970; Amos, 1975) adapted for a VAX 11/780 computer. High density represents greatest exclusion of stain. Scale bar 5 nm. **(b)** Computed projection normal to the filament axis, using the same data as for the cross-section in **(a)**. In this case white corresponds to exclusion of stain to facilitate comparison with original images of negatively stained filaments. The longitudinal pattern within a loop, with three white striations changing to four, is clearly visible. Scale bar 50 nm.

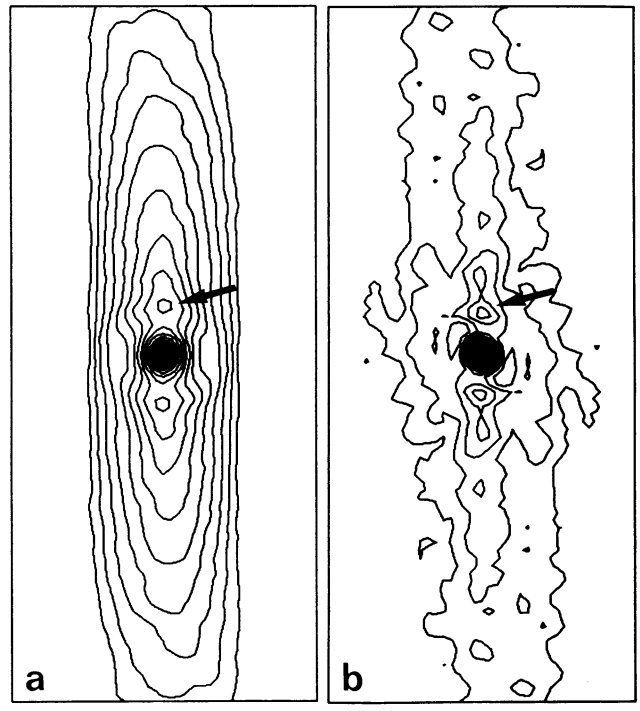

Fig. 5. Autocorrelation maps of paired helical filaments. Some images show hints of transverse striping but the details are never sufficiently coherent to show up in diffraction patterns. The periodicity can still be detected by computing from the images their autocorrelation functions, which display the vector spacings of features in the images. **(a)** and **(b)** are respectively the autocorrelation maps of the PHF and ribbon images shown in Figure 1(e) and (f). Besides the strong origin peak, each shows an axially displaced subsidiary peak (arrow) corresponding to axial spacings in the image of ~3 nm.

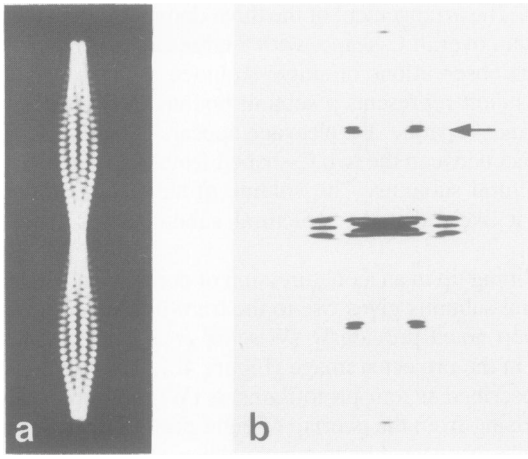

Fig. 6. **(a)** Simulated image of a paired helical filament based on the subunit structure established in this paper. It incorporates a cross-section like that shown in Figure 4a and a subunit spacing of 3 nm as indicated by the autocorrelation function (Figure 5). For the purposes of the present illustration, a symmetry based on a single start helix with a repeat of 104 subunits in 51 turns has been chosen, with a rise per subunit of 1.5 nm. This gives a spacing between neighbouring subunits along a strand of 3 nm and an overall cross-over spacing of 78 nm. The axial resolution in the reconstruction (Figure 4) does not permit one to decide whether the subunits are arranged on a 1- or 2-start helix. The use of a 1-start helix together with an axial kinking of each subunit gives rise to a staggered pattern of transverse striations like that sometimes seen in small regions of filament. **(b)** Computed diffraction pattern of **(a)** showing that, besides the low order layer lines, there is only a small group of layer lines at 1/3 nm^{-1} (arrowed) and a meridional reflection at 1/1.5 nm^{-1}. The pattern is otherwise empty, making complete indexing of diffraction patterns from real images difficult, as the variability in transverse striping blurs out the 1/3 nm^{-1} layer lines.

lines, there is only a set of layer lines in the region of 1/3 nm^{-1} and a weak meridional spot at 1/1.5 nm^{-1}. This general appearance is very like that found in transforms of real images and means that it is difficult to index the whole pattern reliably. It is for this reason that the detection of the axial spacing by the autocorrelation function proved useful. We have also used the model data to check on the axial smearing produced by using only the low order layer lines and find that it has a negligible effect on the computed cross-section.

The present structural data, taken in conjunction with our previous observations, are not consistent with proposals that PHFs might arise from the collapse (Sato *et al.*, 1982), or helical aggregation (Metuzals *et al.*, 1981), or cross-linking (Selkoe *et al.*, 1982a, 1982b) of preformed cytoskeletal polymers, such as neurofilaments, actin, microtubules or their constituent protofilaments. In particular the fragmentation patterns of PHFs (Wischik *et al.*, 1985) are quite unlike the unravelling of α-helical coiled-coils seen when intermediate filaments are treated with appropriate buffers (Aebi *et al.*, 1983). The architecture of PHFs is more akin to the actin-containing microfilaments, in having an axially compact subunit helically arranged to give a two-stranded morphological appearance. However, the symmetry, dimensions and substructure of PHFs are quite different from microfilaments. Furthermore the structure of the PHF subunit and of the PHF itself are quite unlike that of the tubulin dimer and of the assembled microtubule. It is therefore unlikely that the process of tangle formation has any immediate analogy with the perikaryal aggregates of cytoskeleton formed after microtubule depolymerisation.

Whether or not the subunit has biochemical homology with any of the cytoskeletal proteins is unknown. Recent immunocytochemistry (Perry *et al.*, 1985) has suggested that free PHFs can be decorated with antibodies directed against microtubule-associated proteins (MAPs) and against neurofilament antigens found in the side-arm of the 210-kd neurofilament component. There is however no compelling evidence that either a MAP or a neurofilament protein are intrinsic to the core structure of the PHF. Masters *et al.* (1985) on the other hand have observed that some tangles can be labelled in histological sections with antibodies raised against Alzheimer plaque core amyloid, but give no evidence of PHF decoration with the antibodies. The antibodies recognise a 4-kd peptide and it is argued that PHFs, like vascular and plaque core amyloid, are constructed from the same subunit. However, the morphology of amyloid fibrils is quite distinct from that of PHFs (Merz *et al.*, 1983). Moreover the PHF subunit we have defined structurally has a volume corresponding to a protein of mol. wt. >200 kd. It is hard to understand how such a large structural subunit could be formed entirely from the small 4-kd peptide described by Masters *et al.* (1985). The biochemical nature of the PHF must therefore still be regarded as an open question.

Our new structural data are consistent with a picture in which PHFs arise from the *de novo* assembly of a large subunit to form aberrant polymers. The subunit appears to be produced in considerable abundance in those neurons where tangles form. It remains to be established whether the protein is newly synthesized in tangle-bearing neurons, or whether it arises for instance by post-translational modification of a normal constituent. Clearly the unequivocal characterization of the biochemical nature of the three-domained subunit we have demonstrated structurally, and the factors which drive and stabilize its assembly into PHFs, will be crucial for defining a fundamental molecular lesion in Alzheimer's disease.

Materials and methods

Preparation and electron microscopy of PHFs

All preparative protocols and procedures for electron microscopy were exactly as described previously (Wischik *et al.*, 1985). Briefly, the brains were obtained post-mortem from well-documented cases with a clinical diagnosis of senile dementia of the Alzheimer type. The diagnosis was confirmed histologically by the presence of large numbers of plaques and tangles in frontal and temporal cortex. Material was taken from frontal and temporal cortex and hippocampus and tangle fragments were prepared by a series of differential centrifugations in non-denaturing conditions. For electron microscopy the resuspended final pellet was placed on a 400-mesh carbon-coated grid and stained with lithium phosphotungstate (pH 6.0). Micrographs were recorded at 80 kV at a nominal magnification of 45 000× using a Philips EM301 electron microscope.

Re-interpolation of the images

Because of the variability of twist observed even in apparently well preserved filaments, and because of filament curvature, it has proved difficult to obtain interpretable optical diffraction patterns directly from the images of PHFs. Accordingly we have used computer methods to straighten filaments and to reduce the variability in helical periodicity. After preliminary digitization of the image at a sampling corresponding to ~0.45 nm on the specimen, an interactive program (written by Dr E.H.Egelman) for an AED 767 raster graphics display was used to straighten the filaments. The program fits a cubic spline to the plotted curved axis of the particle, and then re-interpolates all the image data points so as to straighten this line. Variations in helical periodicity were removed by re-interpolating individual loops axially to a constant loop length and then re-joining these loops to remake an image of the filament. The effect of this latter re-interpolation is to improve the low resolution part of the computed diffraction pattern, at the expense of smearing out finer axial details. By combining both of these image modifications, it has been possible to visualise reproducibly the first four layer lines of the 80-nm cross-over spacing, whereas only the first order could generally be seen in optical diffraction patterns.

Acknowledgements

We thank Claudio Villa for photographic assistance and Dr A.Klug and Sir Martin Roth for advice and encouragement. CMW is a Meres Senior Student at St. John's College, Cambridge, and a Lister Institute Research Fellow.

References

Aebi,U., Fowler,W.E., Rew,P. and Sun,T.T. (1983) *J. Cell Biol.*, **97**, 1131-1143.
Amos,L.A. (1975) *Proc. Electron Microsc. Soc. Am.*, **33**, 290-291.
Anderton,B.H., Breiberg,D., Downes,M.J., Green,P.J., Tomlinson,B.E., Ulrich,J., Wood,J.N. and Kahn,J. (1982) *Nature*, **298**, 84-86.
Bignami,A., Selkoe,D.J. and Dahl,D. (1984) *Acta Neuropathol.*, **64**, 243-250.
Blessed,G., Tomlinson,B.E. and Roth,M. (1968) *Br. J. Psychiatr.*, **114**, 797-811.
Crowther,R.A., Wischik,C.M. and Stewart,M. (1985) *Proc. Electron Micros. Soc. Am.*, **43**, 734-737.
DeRosier,D.J. and Moore,P.B. (1970) *J. Mol. Biol.*, **52**, 355-369.
Elliott,A., Lowy,J. and Squire,J.M. (1969) *Nature*, **219**, 1224-1226.
Gambetti,P.G., Shechet,G., Getti,B., Hirano,A. and Dahl,D. (1983) *J. Neuropathol. Exp. Neurol.*, **42**, 69-79.
Goldman,R.D., Chojnacki,B., Goldman,A.E., Starger,J., Steinert,P., Talian,J., Whitman,M. and Zackroff,R. (1979) *Neurosci. Res. Prog. Bull.*, **19**, 59-82.
Ihara,Y., Nukina,N., Sugita,H. and Toyohura,Y. (1981) *Proc. Jap. Acad.*, **57**, 152-156.
Iqbal,K., Wisniewski,H.M., Shelanski,M.L., Brostoff,S., Liwnicz,B.M. and Terry,R. (1974) *Brain Res.*, **77**, 337-343.
Iqbal,K., Zaidi,T., Thompson,C.H., Merz,P.A. and Wisniewski,H.M. (1984) *Acta Neuropathol.*, **62**, 167-177.
Kidd,M. (1963) *Nature*, **197**, 192-193.
Kidd,M. (1964) *Brain*, **87**, 307-320.
Masters,C.L., Multhaup,G., Simms,G., Pottgiesser,J., Martins,R.N. and Beyreuther,K. (1985) *EMBO J.*, **4**, 2757-2763.
Merz,P.A., Somerville,R.A. and Wisniewski,H.M. (1983) in Court,L.A. (ed.), *Virus Non-conventionels et Affections du Système Nerveux Central*, Masson, Paris, pp. 259-281.
Metuzals,J., Montpetit,V. and Clapin,D.F. (1981) *Cell Tissue Res.*, **214**, 455-482.
Perry,G., Rizzuto,N., Autilio-Gambetti,L. and Gambetti,P. (1985) *Proc. Natl. Acad. Sci. USA*, **82**, 3916-3920.
Roth,M. (1971) in Kay,D.W. (ed.), *Recent Developments in Psychogeriatrics*, Hadley Bros., Kent, UK, pp. 1-18.
Roth,M., Tomlinson,B.E. and Blessed,G. (1967) *Proc. R. Soc. Med.*, **60**, 254-260.
Sato,Y., Kim,S.U. and Ghetti,B. (1982) *J. Neuropathol. Exp. Neurol.*, **41**, 341.
Selkoe,D.J., Abraham,C. and Ihara,Y. (1982a) *Proc. Natl. Acad. Sci. USA*, **79**, 6070-6074.
Selkoe,D.J., Ihara,Y. and Salazar,E.J. (1982b) *Science*, **215**, 1243-1245.
Tomlinson,B.E. (1982) *Psychol. Med.*, **12**, 449-459.
Wilcock,G.K. and Esiri,M.M. (1982) *J. Neurol. Sci.*, **56**, 343-356.
Wischik,C.M., Crowther,R.A., Stewart,M. and Roth,M. (1985) *J. Cell Biol.*, **100**, 1905-1912.
Wisniewski,H.M. and Terry,R. (1970) in Wolstenholme,G.W. and O'Connor, M.O. (eds.), *Alzheimer's Disease and Related Conditions*, Churchill, London, pp. 223-248.
Wisniewski,H.M., Narang,H.K. and Terry,R.D. (1976) *J. Neurol. Sci.*, **27**, 173-181.
Wisniewski,H.M., Merz,P.A. and Iqbal,K. (1984) *J. Neuropathol. Exp. Neurol.*, **43**, 643-656.
Wisniewski,K., Jervis,G.A., Moretz,R.C. and Wisniewski,H.M. (1979) *Ann. Neurol.*, **5**, 288-294.

Received on 30 September 1985; revised on 31 October 1985